New Dataset of Atmospheric Parameters Retrieved by PFS-MEx

M. Giuranna and the PFS Team (marco.giuranna@iaps.inaf.it)

Istituto di Fisica dello Spazio Interplanetario INAF-IFSI, Via del Fosso del Cavaliere 100, 00133 Roma, Italy.

Introduction

We used thermal-infrared spectra returned by the Mars Express Planetary Fourier Spectrometer (PFS/MEx) to retrieve atmospheric temperature profiles, surface temperatures, and column-integrated optical depths of dust and water ice. More than 2,500,000 spectra were processed to build this new atmospheric dataset, covering the full range of season, latitude, longitude, and local time. The data presented here span more than six Martian Years (from MY 26, Ls = 331°, 10 January 2004 to MY 33, Ls = 78°, 6 December 2015). Atmospheric temperatures and aerosols opacity are successfully retrieved in the polar regions, including the polar nights. By exploiting PFS/MEx capability to perform observations at different local times (LT), this dataset allows investigation of the daily cycles of suspended dust and ice. We present an overview of the seasonal and latitudinal dependence of atmospheric quantities during the relevant period, as well as an assessment of the interannual variability in the current Martian climate. Local time variations of Martian aerosols are also presented, including dust daily cycles during non-dusty seasons and during the global dust storm of MY 28, and daily variation of water ice opacity in the aphelion cloud belt. The general effect of suspended dust on atmospheric temperatures observed during the global dust storm of MY 28 is also presented. With unprecedented spatial and temporal coverage, and details revealed, this dataset offers new challenges to the Martian global circulation models and, at the same time, a new reference for the MYs complementary to those observed by MGS-TES.

PFS Dataset and Retrevals

Here we present the dataset of atmospheric parameters retrieved by PFS for more than 6 full MYs. We used PFS data collected from Ls = 331° of MY26 (January 10th, 2004) to Ls = 78° of MY 33 (December 6th, 2015) to derive surface temperatures, vertical temperature profiles, and integrated dust and ice content in the Martian atmosphere. The zonally-averaged values of atmospheric temperatures at 0.5 mbar (~ 25 km), as well as of dust and ice opacity as a function of season (Ls) and latitude are shown in **Fig. 1**.

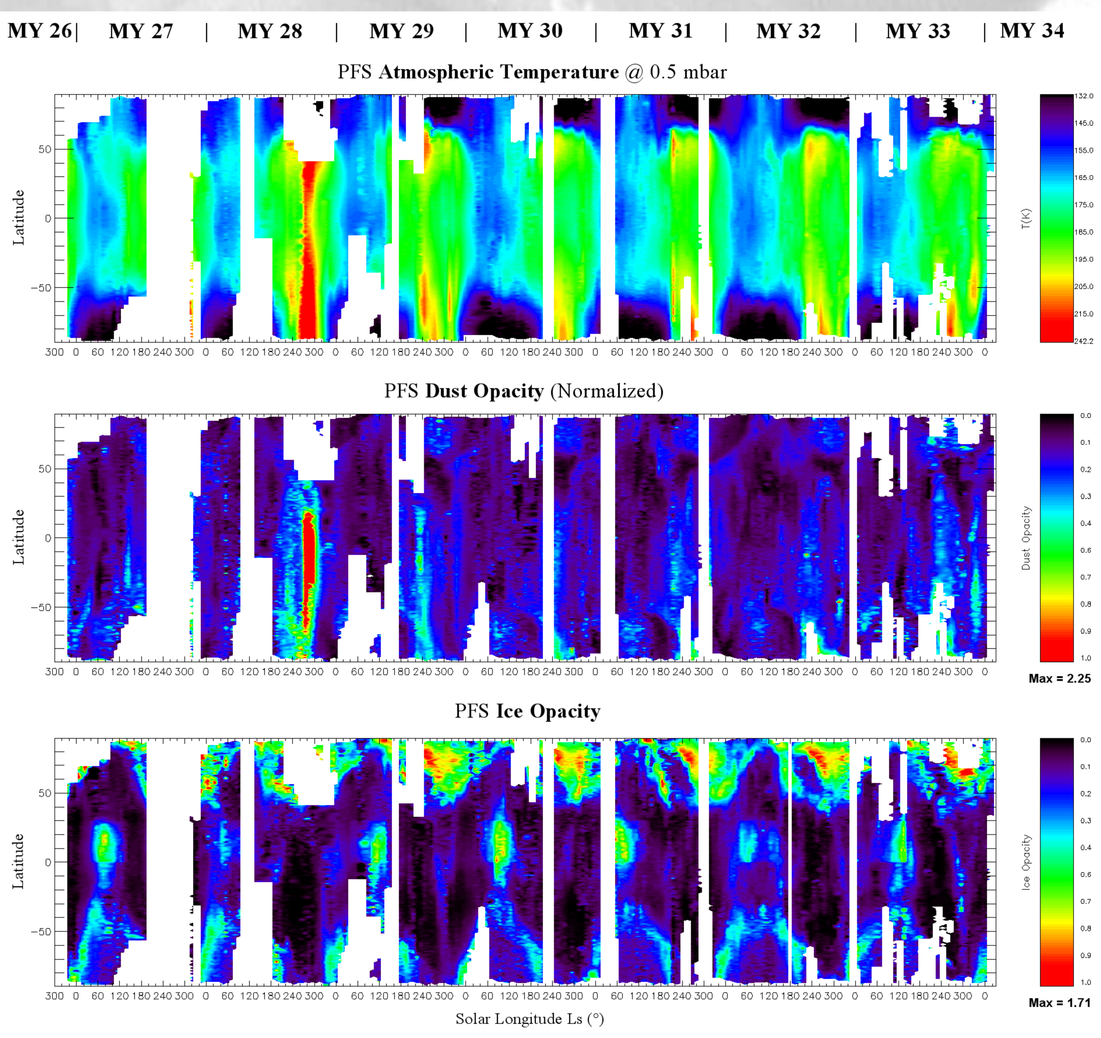

Fig. 1. Zonal-mean atmospheric temperatures at 0.5 mbar (top), integrated dust (middle) and ice (bottom) opacity as a function latitude and Ls for different Martian years. The dust opacity is normalized to a reference pressure level of 6.1 mbar. White areas indicate observational gaps (lack of data) caused by different reasons in the various years of MEx operations, including spacecraft safe modes, spacecraft mass memory issues, solar conjunctions, eclipse seasons, and other spacecraft and PFS temporary issues.

The retrieval algorithm (Grassi et al., 2005; Wolkenberg et al., 2018) makes use of the optimal estimation method coupled with the Bayesian approach, and was optimized for the retrieval of dust and ice opacity during strong dust storms and in the aphelion cloud belt, respectively, as well as over cold surfaces and in the polar nights. Used range 275–1300 cm^{-1}.

The computation of synthetic spectra relies on the DISORT solver implemented in the ARS code, which was specifically developed for the analysis of PFS spectra, and include a full treatment of atmospheric multiple scattering by suspended particles.

Mie theory is used for single-scattering quantities. HITRAN 2012 is used as spectroscopic database for the calculation of the gaseous absorption coefficients. Synthetic spectra are obtained performing the line by line computation and then filtering the result with the PFS instrumental line shape (ILS).

Climatology of water ice clouds

The seasonal and latitudinal variation of water ice cloud optical depth as observed by PFS is shown in **Fig. 2**. Data collected from all observed Martian years were binned in 5° Ls × 1° latitude bins. In contrast to what reported by previous analyses of different datasets, the most prominent feature one can observe is the seasonal extent, pattern and thickness of the NPH, rather than the ACB. Indeed, most of the thickest Martian clouds (on a zonally-averaged sense) are observed in the polar hoods.

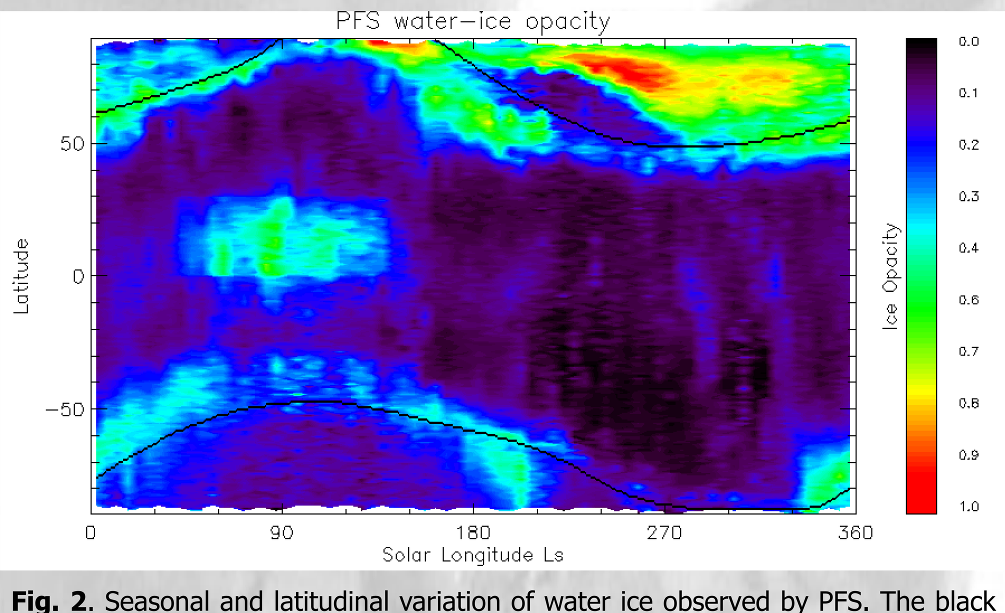

Fig. 2. Seasonal and latitudinal variation of water ice observed by PFS. The black curve shows the climatological latitude of the seasonal CO_2 polar cap edges (Titus, 2005; Titus and Cushing, 2017).

The polar hoods are observed all year long by PFS in both polar regions, although they show very different characteristics. The NPH exhibits larger opacities and always extends to the pole, while the SPH is an optically thinner annular ring that basically follows the climatological latitudes of the seasonal (water) ice cap edge.

The NPH shows peculiar features, observed here for the first time, with characteristic spatial and seasonal patterns that repeat very similarly every Martian year. Large opacities (> 0.5) are always observed at latitudes > 80° N, from the summer solstice (Ls = 90°) until the vernal equinox (Ls = 360°). From 270° to 360° Ls, the whole polar N region is covered with optically-thick water ice clouds.

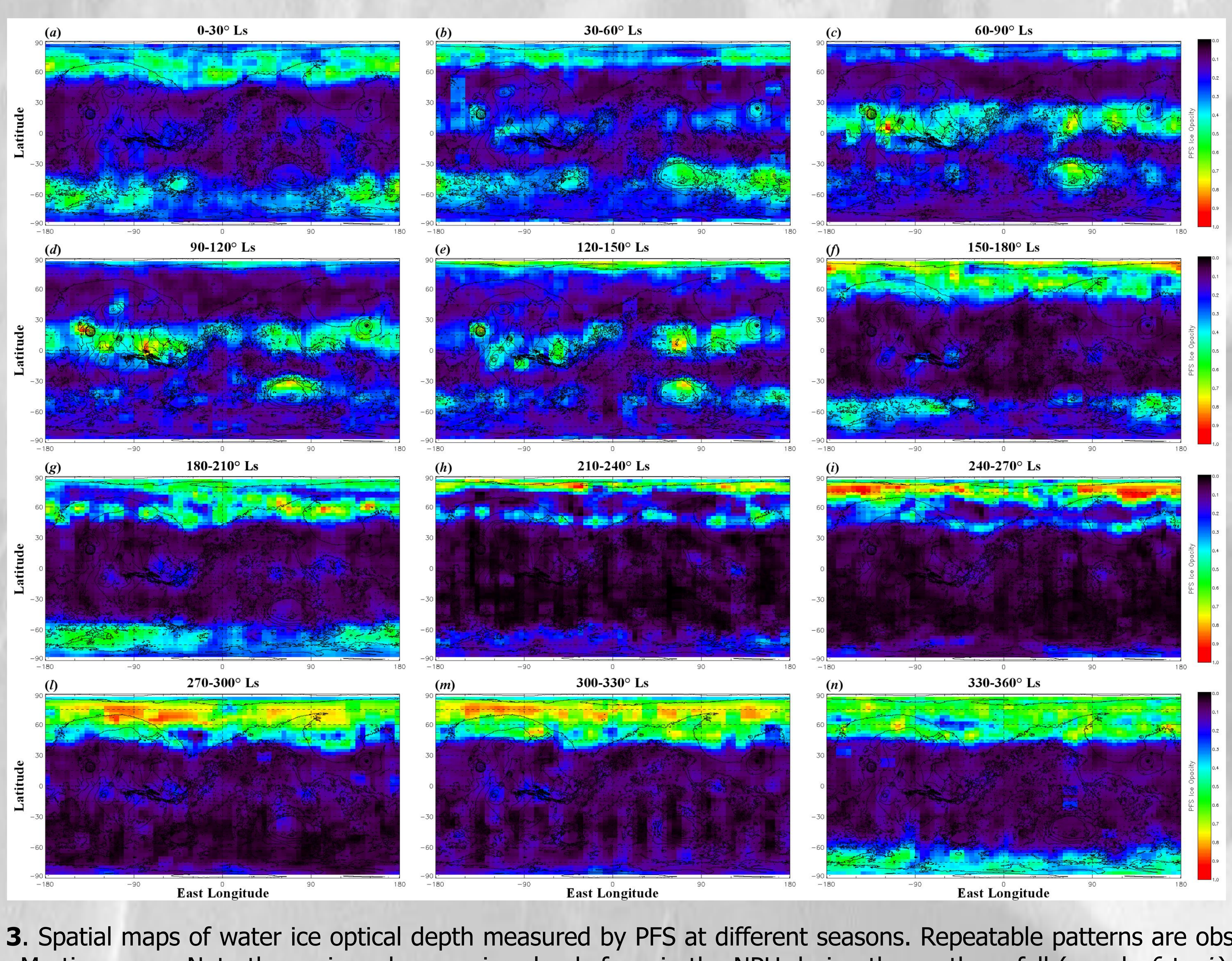

Fig. 3. Spatial maps of water ice optical depth measured by PFS at different seasons. Repeatable patterns are observed every Martian years. Note the region where no ice clouds form in the NPH during the northern fall (panels *f* to *i*). Note also the strong decrease of SPH opacity in correspondence of the period of maximum activity of the aphelion cloud belt (panels *c* to *e*).

The extent of the polar hoods vary with the season. Their boundaries always exceed those of the seasonal CO_2 polar caps in either hemispheres, and rather follow those of the seasonal annuli of water ice observed in both hemispheres by several instruments. In **Fig. 3** we show the spatial distribution of water ice clouds throughout the whole Martian year, in bins of 30 degrees of solar longitude. Data collected from all observed Martian years were binned in 5° longitude × 3° latitude bins. In both hemispheres, the maximum extension is observed around the respective winter solstices, when the SPH boundary reaches ~25° S and the NPH extends down to ~35° N latitude. However, in proximity of the solstices, the polar hoods also show lower opacity.

We consistently observe a region where practically no ice clouds form during the entire northern fall. This "cloud-free" region is observed every Martian year between 170° and 280° Ls. It is always about 60 degrees of solar longitude wide, but moves latitudinally towards lower latitudes as the season advances. It is first observed around 170° Ls and 75° N. Then, it gradually extends and move to lower latitudes with the season, and is finally observed around 50° N in the seasonal interval 220-280° Ls.

Climatology of Dust

In **Fig. 4** we show the latitudinal and seasonal evolution of dust activity on Mars. A region of extremely dust-clear atmosphere separates the dust in the winter tropics from the aerosols (mainly CO_2 ice clouds) in the winter high latitudes. This feature repeats every Martian year and is mainly observed at mid-latitudes (45-60° N) around the northern winter solstice (Ls = 220-310° Ls). It is not reproduced by any of the current GCMs available for Mars and a complete explanation is still missing. The apparent large opacity observed around the winter solstices in both polar regions is actually due to the presence of CO_2 ice clouds.

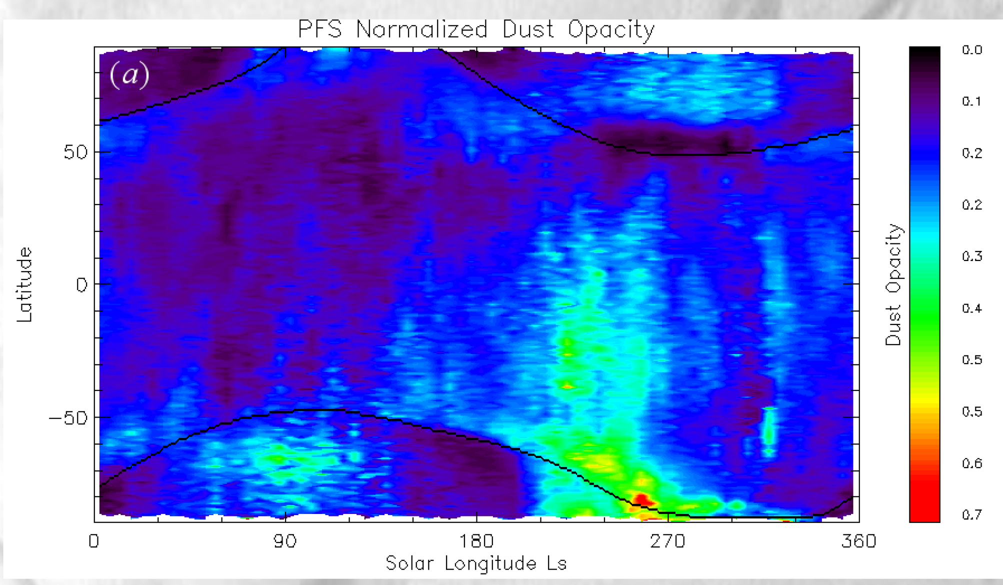

Fig. 4. Seasonal and latitudinal variation of atmospheric dust column opacity observed by PFS (all Martian years except MY 28). 5° Ls × 1° latitude bins. The black curve shows the climatological latitude of the seasonal CO_2 polar cap edges. Note the continuous dust activity at the edges of the seasonal caps in both hemispheres, and the development of strong, planet-encircling dust storms at high southern latitudes in the 210-270° Ls range. Note also the extremely dust-clear atmosphere in the northern mid-latitudes (50-60° N latitude) around the winter solstice (Ls = 240-300°) observed every Martian year.

Daily Cycle of Dust and ice

Dust: Non-dusty seasons. Mean values of dust opacity during non-dusty seasons (Ls < 200° and Ls > 330°) are presented in **Fig. 5** as a function of local time. They were averaged in one-hour bins of local time, separately for the northern (0-40° N) and the southern (0-40° S) hemispheres. The 1-σ error bars in **Fig. 5** provide indication of the combined zonal, meridional, and interannual variations observed.

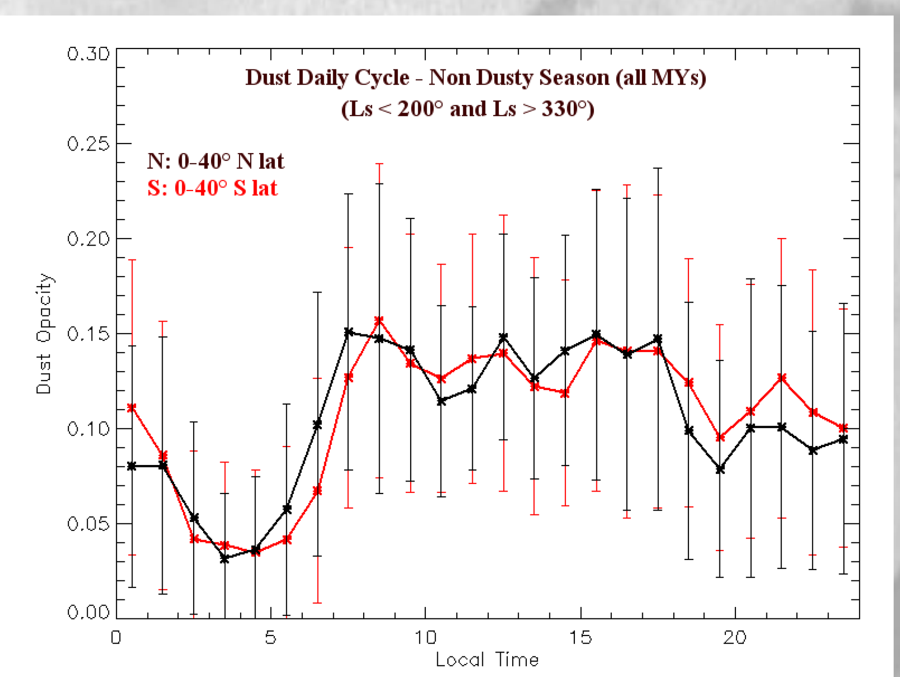

Fig. 5. Daily variation of dust opacity during non-dusty seasons, for the indicated seasonal and latitudinal ranges.

In both hemispheres, the mean dust opacity shows a clear and similar daily cycle. Dayside mean opacity (7 AM – 5 PM) shows constant values ranging between 0.12 and 0.15, in agreement with previous observations at 2-3 PM. The opacity decreases as the sunset approaches (5-6 PM) and a relative minimum is observed in both hemispheres between 7-8 PM. Then, night-time average values around 0.1 are observed up to midnight. After midnight, we consistently observe a rapid decrease of dust opacity. The minimum opacity values are registered in early-morning hours, between 3 AM and 5 AM, when the average column opacity is around 0.03-0.04. As the dawn approaches (5-6 AM), a rapid increase of dust opacity is observed until 7-9 AM, when the mean dayside abundance of suspended Martian dust is restored.

MY 28 Global Dust Storm. In **Fig. 6** we present the mean values of dust opacity observed by PFS during the global dust storm of MY 28 (2007) as a function of local time. Column-integrated dust opacity retrieved by PFS is averaged in one-hour bins of local time, separately for the northern (0-40° N) and the southern (0-40° S) hemispheres.

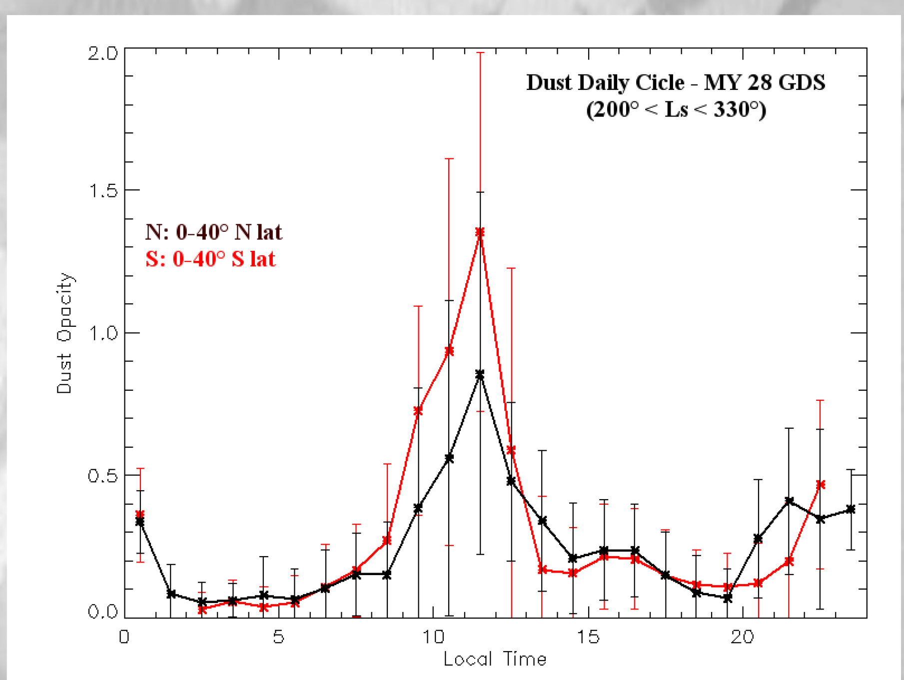

Fig. 6. Daily variation of dust opacity observed by PFS during the global dust storm in MY 28 for the seasonal and latitudinal ranges indicated. The 1-σ error bars provide indication of the observed zonal and meridional variations.

Similarly to the non-dusty season, the lowest opacities (< 0.1) are observed in early morning (1-6 AM), then they start to increase as the dawn approaches (LT ≥ 6 AM). However, a remarkably sharp peak of opacity is consistently observed around midday in both hemispheres. The average dust opacity increases rapidly after 8 AM in both hemispheres, and a large peak-opacity is observed between 11-12 AM. Then, an equally rapid decrease of opacity is observed during the next two or three hours. The peak-opacity is larger in the Southern hemisphere (~1.3-1.4) than in the Northern one (~0.8-0.9), due to a most intense dust activity at the southern latitudes. At 2-3 PM, the dust opacity is already decreased to a value of ~0.2 in both hemispheres. It further decreases as the sunset approaches (5-6 PM) and reaches a minimum value of ~0.05-0.1 at 7-8 PM. Then, after 8 PM, the opacity increases again in both hemispheres to a value of ~0.4 in about two or three hours, only to decrease again after midnight to the low early-morning values observed by PFS.

Ice opacity in the ACB. In **Fig. 7** we present the mean values of ice cloud opacity observed by PFS in the aphelion cloud belt as a function of local time. Column-integrated dust opacity retrieved by PFS between 0-30° N and 50-140° Ls in different Martian years is averaged in one-hour bins of local time. The 1-σ error bars in the figure provide indication of the observed zonal, meridional and interannual variations.

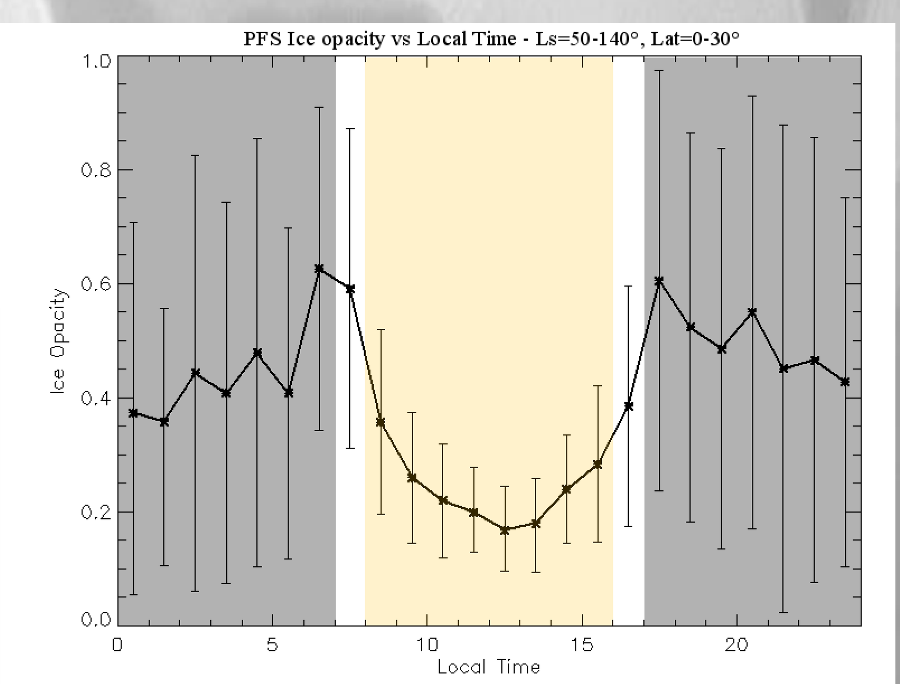

The observed daily cycle of ice opacity shows a nearly symmetric behaviour around noon, when the minimum of opacity is observed. The mean ice opacity increases almost linearly from midnight, when a mean value of 0.4 is observed, to 7 AM, when it peaks to a value of ~0.6. The clouds optical depth then decreases during late morning to a minimum of 0.2 around local noon, and increases again during early to mid afternoon to reach a maximum value of 0.6 around 6 PM, similar to that observed in the morning. Then, the ice opacity decreases almost linearly from late afternoon until midnight.

Fig. 7. Daily variation of water ice opacity observed by PFS in the aphelion cloud belt, for the indicated seasonal and latitudinal ranges.

Data Assimilation

Cons: Sparse coverage -> Only few observations per day. Possible mitigation: multi-datasets assimilation; interpolation.
Pros: First-time full coverage of polar regions, cold surfaces, polar nights. Observations at all local times.